

High-Resolution Spectroscopy on the Laser-Cooling Candidate La^-

E. Jordan,^{1,*} G. Cerchiari,¹ S. Fritzsche,^{2,3} and A. Kellerbauer¹

¹Max-Planck-Institut für Kernphysik, Saupfercheckweg 1, 69117 Heidelberg, Germany

²Helmholtz Institute Jena, Fröbelstieg 3, 07743 Jena, Germany

³Theoretisch-Physikalisches Institut, Friedrich-Schiller-Universität Jena, 07743 Jena, Germany

(Received 20 May 2015; published 8 September 2015)

The bound-bound transition from the $5d^26s^2\ ^3F_2^e$ ground state to the $5d6s^26p\ ^3D_1^o$ excited state in negative lanthanum has been proposed as a candidate for laser cooling, which has not yet been achieved for negative ions. Anion laser cooling holds the potential to allow the production of ultracold ensembles of any negatively charged species. We have studied the aforementioned transition in a beam of negative La ions by high-resolution laser spectroscopy. The center-of-gravity frequency was measured to be 96.592 80(10) THz. Seven of the nine expected hyperfine structure transitions were resolved. The observed peaks were unambiguously assigned to the predicted hyperfine transitions by a fit, confirmed by multiconfigurational self-consistent field calculations. From the determined hyperfine structure we conclude that La^- is a promising laser cooling candidate. Using this transition, only three laser beams would be required to repump all hyperfine levels of the ground state.

DOI: 10.1103/PhysRevLett.115.113001

PACS numbers: 32.80.Gc, 32.30.Bv, 37.10.Rs

Despite the importance of anions in many research fields ranging from plasma physics to atmospheric science and astrophysics [1–3], they cannot currently be studied at ultracold temperatures. Presently available cooling techniques, involving electron, buffer gas, or resistive cooling [4–6] limit the achievable temperature to that of the surrounding environment, typically a few kelvins. The recently suggested technique of anion laser cooling [7] holds the potential to overcome that restriction and to allow the production of ultracold ensembles of any negative ion species by sympathetic cooling. However, until recently no atomic anions with suitable strong electric-dipole transitions were known to exist.

Atomic anions also play an important role as model systems to better understand the correlation effects in complex atomic systems [8,9]. They exhibit an enhanced sensitivity to electron–electron correlations due to the screening of the nucleus by the atomic electrons [10]. Although systematic spectroscopic studies on negative ions have been carried out for several decades [11–13], their structure remains poorly characterized. This is because negative atomic ions are weakly bound systems. Their low binding energy sustains only few, if any, bound excited states. Often, these levels belong to the same fine structure multiplet; hence, transitions between them are dipole forbidden and have low transition rates.

Recent years have seen a renewed interest in negative ions, focusing on those ions with dipole transitions to *bound* excited states. The discovery of the first bound-bound electric-dipole transition in an atomic anion, in Os^- [14], triggered a series of theoretical and experimental investigations. Our group has carried out a thorough study of the osmium anion by high-resolution laser spectroscopy

[15–18]. Among other issues, the absorption cross section of the potential laser cooling transition in Os^- was found to be too low for fast cooling. Recent relativistic-configuration interaction calculations predict that a bound-bound transition in negative lanthanum does not suffer from this shortcoming [19,20].

In particular, the transition between the $5d^26s^2\ ^3F_2^e$ ground state (binding energy ≈ 470 meV [21]) and the $5d6s^26p\ ^3D_1^o$ excited state was identified as particularly well suited due to the high decay rate of the excited state and its large branching ratio back to the ground state [19]. An experimental survey using photodetachment spectroscopy with a tunable pulsed optical parametric oscillator (OPO) showed that several strong lines exist, including bound-bound transitions [22]. Twelve resonances in the energy range 259–539 meV were identified and assigned to the calculated levels of Ref. [19]. The proposed laser cooling transition was observed at 96.5786(73) THz (excitation energy ≈ 399 meV).

Because of the nuclear spin $I = 7/2$ of the stable isotope ^{139}La , this transition exhibits hyperfine structure (HFS), neglected in the aforementioned calculations and unresolved in the prior experimental survey. However, in order to identify the specific hyperfine transition(s) most suitable for laser cooling, the full HFS as well as the relative strengths of all hyperfine transitions must be determined. For this purpose, we carried out high-precision laser spectroscopy on a beam of La^- ions with an unprecedented precision of ≈ 100 MHz. We resolved the HFS, determined the relative transition strengths, and unambiguously assigned the observed peaks to individual hyperfine transitions. The results presented in this Letter suggest that La^- is an excellent candidate for anion laser cooling.

The measurements were performed at the Max Planck Institute for Nuclear Physics (MPIK). The experimental setup has been described in detail elsewhere [15]. Briefly, as shown in Fig. 1 (top), an anion beam is produced with a Middleton-type sputter ion source and accelerated to kinetic energies $E_{\text{kin}} = 5\text{--}10$ keV. The La^- ions are mass-separated from other elements and contaminant molecules in a dipole magnet with a resolving power of $m/\Delta m \approx 180$. The negative ions are guided into the spectroscopy section [Fig. 1 (bottom)] by a 90° electrostatic deflector [23]. The collinearly overlapping ion and laser beams interact in a volume defined by two diaphragms (diameters 7.5 mm, distance 758 mm).

In resonance, the excitation laser brings the ions into the $^3D_1^o$ excited state. If they absorb a second photon, they are neutralized by photodetachment [24]. A deflector guides the remaining ions into a Faraday cup, while neutral atoms are detected by a channeltron detector. The excitation and detachment laser beams originate from the same laser source. The detachment beam is introduced anticollinearly with a slight angle of at most 1° ; its frequency is shifted out

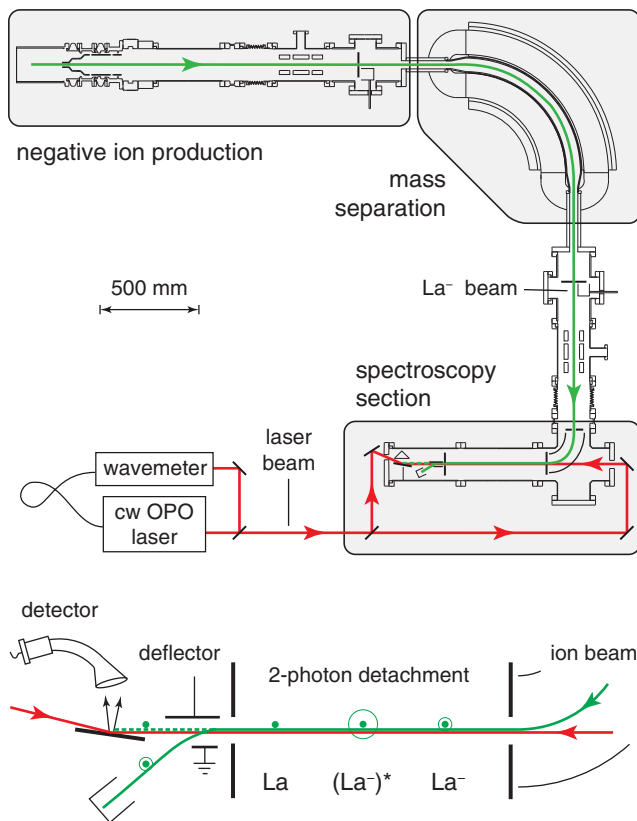


FIG. 1 (color online). (Top) Overall sketch of the spectroscopy setup in operation at MPIK. (Bottom) Spectroscopy section with two laser beams (red lines), one for the excitation (from right) and the other, with higher power, for photodetachment (from left). The green line is the ion beam, and the dotted green line represents neutrals produced by two-photon detachment going straight onto the detector.

of resonance by 50–80 GHz due to the Doppler effect. The mirror used to introduce the detachment laser beam also acts as secondary-electron emitter. The two laser beams can be reversed in order to switch between (anti-)collinear configurations.

The laser light was produced by a continuous-wave OPO (Argos Aculight 2400 with Module B) pumped by a fiber amplifier, in turn seeded by a fiber laser. The tuning range of the idler output is 2600–3200 nm, its bandwidth is <1 MHz. The wavelength of the idler is determined by measuring those of the signal and the pump beams with a wave meter (HighFinesse WS Ultimate 30-IR) calibrated with a stabilized diode laser (HighFinesse SLR-1532). The power of the excitation beam was 2–60 mW (intensity 45–1360 W/m²), that of the detachment beam 1 W (2×10^4 W/m²). For background subtraction, each laser beam was periodically interrupted with a chopper. The data were normalized both to the laser power and to the ion beam current, which typically decreased from ≈ 40 to ≈ 5 pA over 48 h [25].

A typical hyperfine spectrum, recorded at 5 keV beam energy, is shown in Fig. 2. The seven resolved transition peaks were fitted with seven Lorentzians using a nonlinear least-squares fit. The width of the peaks for the spectrum in Fig. 2 was found to be $\Gamma = 75(1)$ MHz for peaks 1–6 and $\Gamma = 114(3)$ MHz for peak 7. The width is a complex function of velocity bunching [26], as well as Doppler and power broadening. The Doppler broadening has two contributions, one due to the temperature of the target and another due to a variation of the acceleration potential

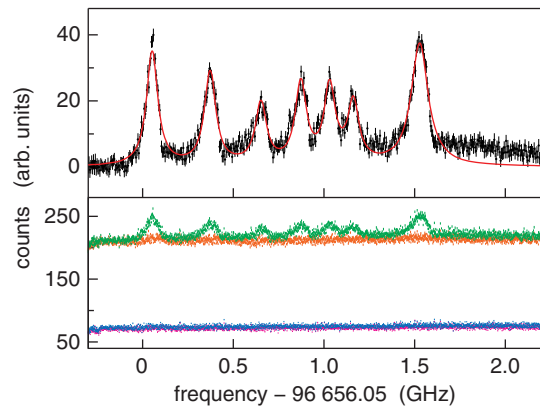


FIG. 2 (color online). (Top) Hyperfine spectrum measured at 5 keV beam energy. The plot is obtained by subtracting the orange and the blue traces from the sum of the green and the magenta traces in the lower pane. The solid red line is a fit of seven Lorentzians. The peak heights and positions are free fit parameters; the widths are forced identical for peaks 1–6. (Bottom) Measured counts of neutral La normalized by ion beam current. The magenta trace represents the counts with both lasers blocked; the blue trace with excitation laser only; the orange trace with detachment laser only; the green trace with both lasers on.

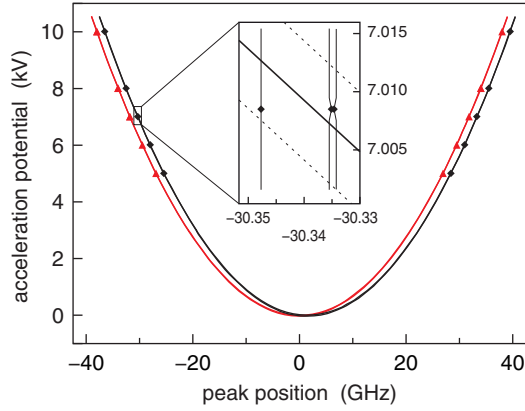


FIG. 3 (color online). Beam energies as a function of the measured Doppler-shifted frequencies of peak 1 (red triangles) and peak 7 (black diamonds). Collinear and anticollinear configurations lead to blue- and redshifted frequencies, respectively. The data for each peak were fitted with parabolas. The minima correspond to the rest frequencies. The inset shows three data points for peak 7 at 7 keV beam energy, as well as the 1σ confidence bounds in addition to the quadratic fit.

perceived by the ions because the location of production varies. The convolution of these effects leads to the observed Lorentz or Voigt line shape.

In all records, a total of seven peaks were observed and numbered in order of increasing frequency. All peaks were slightly asymmetric, with a tail towards higher (lower) frequency for red(blue)shifted resonances. This tail is caused by the excitation of ions inside the electrostatic deflector, where they still have a radial velocity component. It is also responsible for the observed background. All 16 recorded spectra were fitted as described above. The uncertainties of the count rate were increased until $\chi^2 = 1$ for the Lorentzian fits to account for the asymmetric peak shapes. The determined frequencies were then plotted as a function of the kinetic energy, as shown in Fig. 3. Uncertainties of the acceleration potential were expanded

to account for the uncertainties in frequency. The data were then fitted with a quadratic fit, according to the well-known Doppler shift formula, to extract the transition frequencies in the ions' rest frame. The resulting parabolas for peak 1 and peak 7 are also shown in the figure.

All results are summarized in Table I. The systematic uncertainties of the frequencies in the rest frame of the ions comprise the uncertainty of the wave meter (50 MHz), as well as uncertainties of the ion-optical potentials and the mass separator current. These latter two effects were estimated from SimIon simulations and found to contribute less than 1 MHz. Both the asymmetric shape of the resonance due to the electrostatic deflector and the overlap between the peaks due to power broadening depend on the intensity of the excitation laser. The magnitude of these two effects was estimated by repeating the measurement at various laser powers and was found to contribute a systematic uncertainty of 30 MHz.

The transition strengths were obtained from averaging the amplitudes of the Lorentzian fits [27]. The observed peak widths depend on the excitation laser intensity and range from 53 to 200 MHz for peaks 1–6 and from 57 to 152 MHz for peak 7. On an absolute scale, the frequency of peak 1 was found to be 96.592 004(86) THz. Weighting the individual frequencies with the fitted peak heights determined at low laser power, the center of gravity of the spectrum was found to be $\nu_0 = 96.592\ 80(10)$ THz from the parabolic fits. Our result agrees with the prior measurement of Ref. [22] within 2σ and improves its precision by almost 2 orders of magnitude.

In order to help interpret the structure of the observed hyperfine spectrum, detailed *ab initio* calculations were performed on the low-lying levels of La^- within the framework of the multiconfiguration Dirac–Fock (MCDF) method. They show that electronic correlations play a very significant role and that systematically enlarged expansions of the many-electron wave functions are required to reproduce observations. For example, to isolate the correct

TABLE I. Relative peak heights (column 4) and relative transition frequencies (column 6) of the measured peaks, with respect to peak 1 at 96.592 004(80) THz. The total angular momentum quantum numbers F of the ground state (1) and the excited state (2) are given in columns 2 and 3, the calculated relative transition amplitudes in column 5. The relative transition frequencies calculated from the fitted A and B parameters are indicated in column 7. The relative transition frequencies from MCDF calculations are given in column 8. See the text for details on the applied scaling.

| Peak number | F_1 | F_2 | a_{expt} | a_{theor} | ν_{expt} (MHz) | ν_{fit} (MHz) | ν_{theor} (MHz) |
|-------------|-------|-------|-------------------|--------------------|---------------------------|--------------------------|----------------------------|
| 1 | 11/2 | 9/2 | 1.00(11) | 1 | 0.0(5.8) | 0.0(4.4) | 0 |
| 2 | 9/2 | 7/2 | 0.77(8) | 0.83 | 324.8(5.8) | 325.9(2.4) | 336 |
| 3 | 7/2 | 5/2 | 0.51(6) | 0.67 | 604.1(5.9) | 604.2(3.8) | 633 |
| 4 | 9/2 | 9/2 | 0.81(8) | 0.83 | 825.1(5.8) | 828.6(3.4) | 817 |
| 5 | 7/2 | 7/2 | 0.74(8) | 0.67 | 990.1(5.9) | 984.3(2.1) | 1006 |
| 6 | 5/2 | 5/2 | 0.53(7) | 0.50 | 1116.2(6.1) | 1104.2(4.1) | 1153 |
| 7a | 3/2 | 5/2 | | 0.33 | | 1454.9(6.9) | 1525 |
| 7b | 5/2 | 7/2 | 1.08(10) | 0.50 | 1480.2(5.8) | 1484.4(2.6) | 1527 |
| 7c | 7/2 | 9/2 | | 0.67 | | 1487.0(3.2) | 1487 |

$5d^26s^2\ ^3F_2^e \rightarrow 5d6s^26p^3\ ^3D_1^o$ transition, computations were first carried out to identify the correct level order. Their main interest concerned the question why only seven (out of nine) hyperfine transitions are observed, and how the lines split and overlap.

To better understand how different wave function expansions affect the splitting of the individual hyperfine-resolved transitions, the RATIP code [28] was extended to directly evaluate the transition energies and rates. While some overlap of the hyperfine transitions already occurs in $5d^26s^2$ and $5d6s^26p$ single-configuration calculations, further computational efforts were required to achieve agreement with experiment for the splitting and the relative intensities of the hyperfine components. Ultimately, both single and double excitations of the $5d$, $6s$, and $6p$ valence electrons into two additional layers of correlation orbitals, together with a proper account of core polarization effects, needed to be taken into account to obtain a proper superposition of the hyperfine components.

Because of the overall negative charge and the three open shells of the La^- ions, it was not possible to directly monitor convergence as the size of the expansions was enlarged. However, from similar computations for neutral Ba [29] and Ra [30] it is known that large-scale calculations are required already for systems with two electrons outside of closed shells, and that the size of the wave function expansions increases very rapidly with additional open shells. From our best approximation for the wave functions of the low-lying 3F_2 and 3D_1 levels, we obtained the relative level splitting of the nine hyperfine components. However, since the nuclear magnetic and electric moments are free parameters in the MCDHF computations, the calculated HFS splitting was *scaled* to the measured positions of peaks 1 and 7c. The result is given in column 8 of Table I and is shown in the lower pane of Fig. 4.

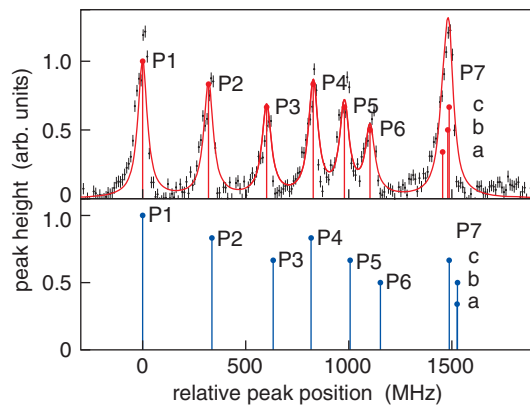


FIG. 4 (color online). Comparison between the hyperfine spectrum determined from the data and the HFS parameter fit (top) and from calculations (bottom). The dots mark the peak heights, the labels the peak numbers. The data in the upper graph were recorded at 10 kV ion beam energy and 2.23 mW laser power. The solid red line is a fit with 9 Lorentzians with a width of 54(1) MHz.

Furthermore, the observed peaks were assigned to transitions between specific HFS levels by a model fit. The angular-momentum quantum numbers are $J = 2$ for the ground state and $J = 1$ for the excited state. Thus the ground state splits into five, the excited state into three hyperfine levels. Therefore, we expect nine allowed hyperfine transitions. The hyperfine splitting can be parametrized by the dipole and quadrupole contributions of a multipole expansion [31], where A and B are the magnetic-dipole and electric-quadrupole hyperfine-interaction constants, respectively. The HFS coefficients were determined by fitting nine Lorentzians to the nine records featuring the highest resolution.

The relative peak heights of the Lorentzians were set to the theoretical values. The width was left as a free parameter, but forced to be the same for all peaks. There is only one set of coefficients that reproduces the observed HFS, with values

$$\begin{aligned} A_{\text{gnd}} &= 146.76(26) \text{ MHz}, & B_{\text{gnd}} &= 36.3(8.8) \text{ MHz}, \\ A_{\text{exc}} &= 110.55(72) \text{ MHz}, & B_{\text{exc}} &= 5.4(1.3) \text{ MHz}, \end{aligned}$$

where the uncertainties are the standard deviations of the nine sets of coefficients. Figure 4 (top) shows a comparison between a spectrum at 10 kV beam energy with the peak positions from the fit. The peak order from low to high frequency is very well reproduced by the fit. It also agrees with the calculated splitting, from which it only differs (within uncertainties) for the closely clustered peaks 7a–7c.

The present spectroscopic results on the La^- HFS lead to the energy level diagram shown in Fig. 5, which can be used to develop a laser cooling scheme. Cooling can be achieved by exciting ions from the $F = 9/2$ and $11/2$ hyperfine levels of the $^3F_2^e$ ground state to the $F = 9/2$ hyperfine level of the $^3D_1^o$ excited state. In addition, the $F = 3/2, 5/2$, and $7/2$ hyperfine levels of the ground state must be repumped in order to prevent losses in the cooling cycle. The figure indicates that laser cooling can be achieved with only three laser beams since the frequencies

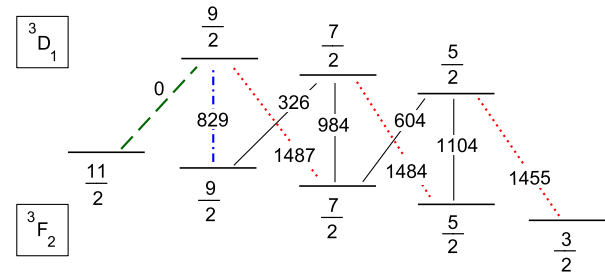


FIG. 5 (color online). Schematic energy level diagram resulting from the HFS fit. The leftmost transition, which is the reference, is at 96.592 004(86) THz, the numbers are the relative transition frequencies in MHz. The red (dotted), green (dashed), and blue (dashed-dotted) colors indicate the three frequencies that are needed to repump all the hyperfine levels of the ground state.

of transitions 7a–7c (red dotted lines in Fig. 5) differ by less than 50 MHz, as evidenced by the fact that they were not resolved in our measurement.

In summary, high-resolution laser spectroscopy on a beam of La^- ions reveals that the potential laser cooling transition from the $5d^26s^2\ ^3F_2^e$ ground state to the $5d6s^26p\ ^3D_1^o$ excited state is split into 9 hyperfine components. We have determined all transition frequencies in the rest frame of the ions and unambiguously assigned the observed features to transitions between the HFS levels of the ground and excited states. From the resulting energy level diagram we conclude that La^- is an excellent candidate for the first laser cooling of anions, assuming the transition rates are as high as theoretically predicted. In addition to the HFS determined in the present work, a knowledge of the absolute transition rates is also required. We will experimentally address this question in the near future.

We thank the MPIK accelerator group and workshop, in particular, M. König, Th. Spranz, and M. Beckmann. Support by J. R. Crespo López-Urrutia with the channeltron detector is gratefully acknowledged. We are indebted to N. D. Gibson, C. W. Walter, and U. Warring for helpful correspondence. This work was supported by the European Research Council (ERC) under Grant No. 259209 (UNIC).

*To whom all correspondence should be addressed.
elena.jordan@mpi-hd.mpg.de

- [1] B. Song, N. D'Angelo, and R. L. Merlino, *Phys. Fluids B* **3**, 284 (1991).
- [2] N. L. Aleksandrov, *Plasma Sources Sci. Technol.* **3**, 226 (1994).
- [3] T. P. Snow and V. M. Bierbaum, *Annu. Rev. Anal. Chem.* **1**, 229 (2008).
- [4] G. Gabrielse, X. Fei, L. A. Orozco, R. L. Tjoelker, J. Haas, H. Kalinowsky, T. A. Trainor, and W. Kells, *Phys. Rev. Lett.* **63**, 1360 (1989).
- [5] D. Gerlich, *Phys. Scr.* **T59**, 256 (1995).
- [6] G. Gabrielse, A. Khabbaz, D. S. Hall, C. Heimann, H. Kalinowsky, and W. Jhe, *Phys. Rev. Lett.* **82**, 3198 (1999).
- [7] A. Kellerbauer and J. Walz, *New J. Phys.* **8**, 45 (2006).
- [8] N. Berrah *et al.*, *Phys. Rev. Lett.* **87**, 253002 (2001).
- [9] L. G. Gerchikov and G. F. Gribakin, *Phys. Rev. A* **77**, 042724 (2008).
- [10] D. J. Pegg, *Rep. Prog. Phys.* **67**, 857 (2004).
- [11] S. J. Buckman and C. W. Clark, *Rev. Mod. Phys.* **66**, 539 (1994).
- [12] C. Blondel, *Phys. Scr.* **T58**, 31 (1995).
- [13] T. Andersen, *Phys. Rep.* **394**, 157 (2004).
- [14] R. C. Bilodeau and H. K. Haugen, *Phys. Rev. Lett.* **85**, 534 (2000).
- [15] U. Warring, M. Amoretti, C. Canali, A. Fischer, R. Heyne, J. O. Meier, Ch. Morhard, and A. Kellerbauer, *Phys. Rev. Lett.* **102**, 043001 (2009).
- [16] A. Fischer, C. Canali, U. Warring, A. Kellerbauer, and S. Fritzsche, *Phys. Rev. Lett.* **104**, 073004 (2010).
- [17] A. Kellerbauer, C. Canali, A. Fischer, U. Warring, and S. Fritzsche, *Phys. Rev. A* **84**, 062510 (2011).
- [18] A. Kellerbauer, A. Fischer, and U. Warring, *Phys. Rev. A* **89**, 043430 (2014).
- [19] S. M. O'Malley and D. R. Beck, *Phys. Rev. A* **81**, 032503 (2010).
- [20] L. Pan and D. R. Beck, *Phys. Rev. A* **82**, 014501 (2010).
- [21] A. M. Covington, D. Calabrese, J. S. Thompson, and T. J. Kvale, *J. Phys. B* **31**, L855 (1998).
- [22] C. W. Walter, N. D. Gibson, D. J. Matyas, C. Crocker, K. A. Dungan, B. R. Matola, and J. Rohlén, *Phys. Rev. Lett.* **113**, 063001 (2014).
- [23] H. Kreckel, H. Bruhns, K. A. Miller, E. Wählin, A. Davis, S. Höckh, and D. W. Savin, *Rev. Sci. Instrum.* **81**, 063304 (2010).
- [24] The binding energy of the excited state in La^- (≈ 70 meV) is too large for electric-field detachment, which was possible for Os^- .
- [25] A. Kellerbauer, G. Cerchiari, E. Jordan, and C. W. Walter, *Phys. Scr.* **90**, 054014 (2015).
- [26] S. L. Kaufman, *Opt. Commun.* **17**, 309 (1976).
- [27] The peak heights depend on the transition amplitudes, the populations of the ground state components and the photo-detachment cross sections of the excited-state components. The latter two are to good approximation equal for all hyperfine sublevels.
- [28] S. Fritzsche, *Comput. Phys. Commun.* **183**, 1525 (2012).
- [29] B. K. Sahoo, *Phys. Rev. A* **74**, 020501(R) (2006).
- [30] J. Bieroń, C. Froese Fischer, S. Fritzsche, and K. Pachucki, *J. Phys. B* **37**, L305 (2004).
- [31] H. Kopfermann, *Kernmomente*, 2nd ed. (Akademische Verlagsgesellschaft, Frankfurt am Main, 1956).